Parametric resonances in a temporal photonic crystal slab

Juan Sabino Martínez-Romero[*] and P. Halevi[†]

Instituto Nacional de Astrofísica, Óptica y Electrónica Tonantzintla, 72840 Puebla, Mexico

We have studied resonances in a dynamic slab whose permittivity and/or permeability are periodic functions of time, namely, a temporal photonic crystal. We find strong and narrow resonances for frequencies that are equal to 1/2 or 3/2, etc. of the modulation frequency provided that a certain geometric parameter (proportional to the slab thickness and to the modulation frequency) assumes values such that the electric field in the slab is either symmetric or antisymmetric with respect to the slab center. These resonances turn out to be absent whenever the electric and magnetic modulations are in phase and have equal strengths, that is, when there are no band gaps between k bands. The resonance peaks appear for all the modulation harmonics and are superimposed on Fabry-Pérot–like background oscillations. For not very strong modulations, the resonances can be described in terms of the relative impedance of the slab and a parameter that expresses the modulation strength.

I. INTRODUCTION

Inspired by duality between space and time, dynamic media—while studied much less than spatially structured media—had aroused interest among numerous scientists for many years. In some cases, this led to finding temporal analogs to diverse, already known, spatial phenomena. For example, the temporal equivalence of reflection and refraction of optical rays at a spatial interface has the principal characteristic that the role of the angle (in the spatial case) is played by frequency shifts at a temporal interface [1]. Using two such temporal interfaces that satisfy the condition of temporal total internal reflection, it is possible to achieve a temporal waveguide that can confine the wave [2,3] even when the central region has a lower refractive index [2]. On the other hand, when a wavefront of a refractive index is generated moving along in a photonic crystal waveguide, it is possible to control photonic transitions [4].

Also, studies were realized of wavelength conversion by means of dynamic adjustment of the index of refraction in a cavity. Unlike other conversion processes, this one is linear, independent of the initial light intensity and is realizable in any material with variable resonance. Moreover, there is no necessity of phase coincidence and the conversion efficiency is near to 100% [5].

Finally, there are also investigations of temporal modulation in the presence of spatial nonuniformity; for example, Ramezani *et al.* [6] show that a temporally modulated spatial defect can cause nonreciprocity, namely allow propagation in one direction, but not in the opposite direction. Lurie *et al.* [7] deal with another system characterized by spatiotemporal variation, having investigated wave amplification in spatiotemporal waveguides. And, according to Ref. [8], the interaction of a wave with a medium that varies in time results in energy interchange between the wave and the medium, enabling either amplification or attenuation of the wave.

The spatiotemporal variations of the permittivity in a medium can be used to design asymmetrically aligned photonic bands in the direction of propagation; thus, with appropriate optical excitation, this system can function as a nonreciprocal optical device [9]. In addition, for oblique incidence of the wave, such structures function as generators of nonreciprocal harmonics and filters [10]. Such effects are of great interest for nonreciprocal systems of antennas [11].

Less than a decade ago, our group initiated the study of temporal photonic crystals, concluding that a medium with permittivity that varies periodically in time gives rise to a photonic band structure of wave-vector bands (k bands), separated by wave-vector gaps (k gaps) [12]. This work has been generalized recently to allow for the periodic modulation in time of the permeability as well [13]. Indeed, the k gaps were observed experimentally for the equivalent system of a modulated, low-pass transmission line [14,15]. Further, in the special case of permittivity modulation, it was shown that resonances in the reflectivity and transmittivity can be obtained if certain conditions are satisfied [16]. In addition, very recently we found that waves whose frequency is one-half of the modulation frequency are stationary [17]. And, in Ref. [18] we also studied pulse propagation through a modulated slab. The present paper generalizes Ref. [16] to include periodic variation in time of the permeability, in addition to the permittivity. We also allow for a possible phase difference between these two modulations, leading to interesting effects. The parametric resonances are derived as solutions of an eigenvalue problem for the dynamic slab, as well as solutions of the optical reflection and transmission response. Also, we develop a convenient and transparent approach for weak modulations that works surprisingly well even for substantial modulations.

This paper is organized as follows. In the following section (II A) we solve the eigenvalue problem for the dynamic slab in
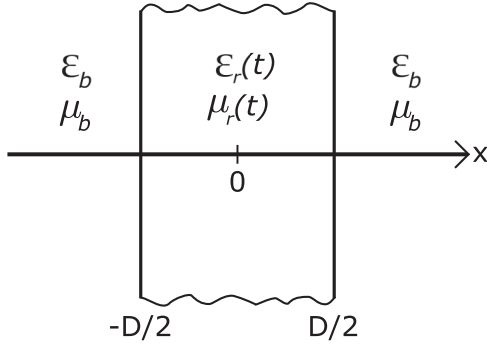
---
[*]jsmr8812@me.com
[†]halevi@inaoep.mx

FIG. 1. Slab whose permittivity and/or permeability are oscillating periodically with time.

Fig. 1 (with no incident wave). Section II B addresses the resonances as solutions of the optical response problem derived in Ref. [13]. Then, in Sec. II C we use the results of Sec. II A to achieve a significant simplification for weak modulations. In Sec. III we compare numerical results obtained from these three methods and explore further an important parameter that controls the resonances. Section IV investigates the reflection and transmission coefficients in the presence of the resonances. Finally, the conclusions are presented in Sec. V.

II. RESONANCES

A. Eigenvalue problem

Our system is defined in Fig. 1: a slab of thickness D whose permittivity and/or permeability are oscillating periodically in time, bounded on both sides by a medium of constant permittivity and permeability. While our theoretical calculations

below are general, for the numerical work (as well as our "weak modulation approximation") we will use the following model for the relative permittivity (dielectric constant) and relative permeability:

$$\varepsilon_r(t) = \bar{\varepsilon}_r[1 + m_\varepsilon \sin(\Omega t)], \tag{1a}$$

$$\mu_r(t) = \bar{\mu}_r[1 + m_\mu \sin(\Omega t + \theta)]. \tag{1b}$$

Here, Ω is 2π times the frequency at which the slab medium is modulated, $\bar{\varepsilon}_r$ and $\bar{\mu}_r$ are the average values of $\varepsilon_r(t)$ and $\mu_r(t)$, and m_ε and m_μ are the corresponding modulation strengths ($0 < m_{\varepsilon,\mu} < 1$). We also allow for the possibility of a phase difference θ between the magnetic and electric modulations.

In this subsection no excitation is assumed ($E_0 = B_0 = 0$), namely, we approach the question of resonance by asking the following: does the system in Fig. 1 support self-sustained oscillations of the electromagnetic fields?

The symmetry of our system implies that the electric field $E(x, t)$ and magnetic induction $B(x, t)$ must be either symmetric or antisymmetric with respect to the center of the slab $x = 0$. Hence they are superpositions of, respectively, $\cos(k_p x)$ or $\sin(k_p x)$, where $p = 1, 2, \ldots$. Here, $k_1(\omega), k_2(\omega), \ldots$ are the wave vectors of the plane waves that can propagate in the dynamic slab at a circular frequency ω [13].

The field $E(x, t)$ in the slab is a superposition of the aforementioned plane waves (implying a summation over the index p). Moreover, both inside and outside the slab, it is a superposition of oscillations with frequencies $\omega - n\Omega$ ($n = 0, \pm 1, \pm 2, \ldots$). The harmonics $\omega \pm \Omega, \omega \pm 2\Omega, \ldots$ are induced by the modulation of frequency Ω [13]. Then we write

$$E(x, t) = \begin{cases} \sum_{p=1}^{\infty} \sum_n E_p f(k_p x) e_{pn} e^{-i(\omega - \Omega n)t}, & |x| \leqslant D/2, \\ \sum_n F_n e^{i(\omega - \Omega n)(\sqrt{\varepsilon_b \mu_b} x/c - t)}, & x \geqslant D/2, \end{cases} \tag{2}$$

where

$$f(k_p x) = \begin{cases} \cos(k_p x), & \text{for symmetric oscillations,} \\ \sin(k_p x), & \text{for antisymmetric oscillations.} \end{cases} \tag{3}$$

From the continuity of $E(x, t)$ at the boundary $x = D/2$ it follows that

$$\sum_n \left[\sum_{p=1}^{\infty} E_p f(k_p D/2) e_{pn} - F_n e^{i(\omega - \Omega n)\sqrt{\varepsilon_b \mu_b} D/2c} \right] e^{-i(\omega - \Omega n)t} = 0.$$

Because this has to be satisfied at every instant t,

$$F_n = e^{-i(\omega - \Omega n)\sqrt{\varepsilon_b \mu_b} D/2c} \sum_{p=1}^{\infty} E_p f(k_p D/2) e_{pn}, \quad n = 0, \pm 1, \ldots. \tag{4}$$

This fixes $E(x, t)$ outside the slab in terms of the (yet undetermined) amplitudes E_p.

The $B(x, t)$ field is found from Faraday's law,

$$\frac{\partial B}{\partial t} = -\frac{\partial E}{\partial x} = \begin{cases} -\sum_{p=1}^{\infty} \sum_n k_p E_p f'(k_p x) e_{pn} e^{-i(\omega - \Omega n)t}, & |x| \leqslant D/2, \\ -\sum_n i(\omega - n\Omega)\left(\frac{\sqrt{\varepsilon_b \mu_b}}{c}\right) F_n e^{i(\omega - \Omega n)(\sqrt{\varepsilon_b \mu_b} x/c - t)}, & x \geqslant D/2, \end{cases} \tag{5}$$

the prime on $f(k_p x)$ implying derivative with respect to the argument.

$$\therefore B(x,t) = \begin{cases} -i \sum_{p=1}^{\infty} \sum_n k_p E_p f'(k_p x) e_{pn} \dfrac{e^{-i(\omega-\Omega n)t}}{\omega - \Omega n}, & |x| \leqslant D/2, \\[2mm] \dfrac{\sqrt{\varepsilon_b \mu_b}}{c} \sum_n F_n e^{i(\omega - \Omega n)(\sqrt{\varepsilon_b \mu_b} x/c - t)}, & x \geqslant D/2. \end{cases} \tag{6}$$

Now we impose the continuity of the magnetic field $H(x,t)$ at $x = D/2$,

$$\frac{B(x = D/2^-, t)}{\mu_0 \mu_r(t)} = \frac{B(x = D/2^+, t)}{\mu_0 \mu_b}, \tag{7}$$

where the periodicity of $\mu_r(t)$ permits the Fourier expansion

$$\mu_r(t) = \sum_n \mu_n e^{in\Omega t}. \tag{8}$$

Then we get that

$$\sum_n \sum_{p=1}^{\infty} \left\{ i k_p f'\left(k_p \frac{D}{2}\right) e_{pn} \frac{1}{\omega - n\Omega} + \frac{1}{c}\sqrt{\frac{\varepsilon_b}{\mu_b}} f\left(k_p \frac{D}{2}\right) \sum_{n'} e_{p(n-n')} \mu_{n'} \right\} e^{in\Omega t} E_p = 0.$$

For this equation to be satisfied for all times t we must have

$$\sum_{p=1}^{\infty} \sum_{n'} \left\{ \frac{1}{c}\sqrt{\frac{\varepsilon_b}{\mu_b}} \mu_{n-n'} f\left(k_p \frac{D}{2}\right)(\omega - n\Omega) + i k_p(\omega) f'\left(k_p \frac{D}{2}\right) \delta_{n'n} \right\} e_{pn'} E_p = 0,$$
$$n = 0, \pm 1, \ldots. \tag{9}$$

This is an eigenvalue equation for the amplitudes E_p; in principle, a set of an infinite number of homogeneous equations for an infinite number of unknowns E_1, E_2, ... for every value of ω.

It is convenient to normalize the frequency ω and the wave vectors k_p by means of the modulation frequency Ω:

$$\hat{\omega} = \frac{\omega}{\Omega}, \tag{10}$$

$$\hat{k}_p = \frac{k_p c}{\Omega \sqrt{\varepsilon_r \bar{\mu}_r}}. \tag{11}$$

We also define the relative average impedance

$$A = \frac{\sqrt{\bar{\mu}_r / \bar{\varepsilon}_r}}{\sqrt{\mu_b / \varepsilon_b}} \tag{12}$$

and the important parameter (proportional to the slab thickness and to the modulation frequency)

$$\nu = D\Omega (\bar{\varepsilon}_r \bar{\mu}_r)^{1/2}/c. \tag{13}$$

In terms of these definitions, Eq. (9) can be now rewritten as

$$\sum_{p=1}^{\infty} \sum_{n'} \left\{ A \hat{\mu}_{n-n'} f\left(\hat{k}_p \frac{\nu}{2}\right)(\hat{\omega} - n) + i \hat{k}_p(\hat{\omega}) f'\left(\hat{k}_p \frac{\nu}{2}\right) \delta_{n'n} \right\}$$
$$\times e_{pn'} E_p = 0, \quad n = 0, \pm 1, \ldots. \tag{14}$$

Here, $\hat{\mu}_n = \mu_n / \bar{\mu}_r$ is the normalized Fourier coefficient of the relative permeability.

In this eigenvalue equation, either the reduced frequency $\hat{\omega}$ or the parameter ν can be assigned an arbitrary value. If a certain value of ν is chosen, Eq. (14) yields eigenvalues for $\hat{\omega}$. On the other hand, selecting a certain value of $\hat{\omega}$, one gets eigenvalues for ν. In Fig. 2 we graph the smallest eigenvalues

of ν as a function of $\hat{\omega}$; these depend on two parameters: the electric modulation m_ε (assuming that $m_\mu = 0$), see Eq. (1), and the average relative impedance A, Eq. (12). It is evident that for all six combinations of m_ε and A chosen, the eigenvalues are strongly centered around $\hat{\omega} = 1/2$ (and, although not shown, also around $\hat{\omega} = 3/2$, $5/2$, etc.). At half height of the peaks, their relative widths $\delta\hat{\omega}/\bar{\hat{\omega}} = 2\delta\hat{\omega}$ are, respectively, 0.0016, 0.0010, 0.0010 for $m_\varepsilon = 0.1$, 0.3, 0.5 with $A = 0.4364$ [Fig. 2(a)] and 0.0016, 0.0016, 0.0014 for $A = 0.2$, 0.4364, 1 with $m_\varepsilon = 0.1$ [Fig. 2(b)]. The fact that $\delta\hat{\omega}/\bar{\hat{\omega}} \ll 1$ confirms the strong localization of our resonances at $\omega = (1/2)\Omega$, $(3/2)\Omega$, ...—just like for parametric resonances in many other situations in science and engineering. However, as is clear from inspection of Fig. 2, there is an additional condition, related to the thickness of the slab, namely, that the parameter ν, Eq. (13), assumes a special value (one of an infinite number that are possible) that depends on two parameter values. Recalling our former paper, Ref. [17], for $\omega = (1/2)\Omega$ [as well as for $\omega = (3/2)\Omega$, $(5/2)\Omega$, ...] the waves are stationary, and we can state that our parametric resonances correspond to stationary waves that are either symmetric or antisymmetric with respect to the slab center. In practice, the resonances are strongest for $\hat{\omega} = 1/2$ so this value will be our starting point and we will seek to determine the ν eigenvalues. We note that the $\hat{k}_p(\hat{\omega})$ and $e_{pn}(\hat{\omega})$ are solutions of the eigenvalue problem for the infinite medium problem [13]. And, because these quantities are periodic (adding an arbitrary integer to $\hat{\omega}$ leaves them unaltered), the same set of eigenvalues ν is obtained for $\hat{\omega} = 1/2$, 3/2, 5/2, ...

B. Optical response

As an alternative approach to the resonance problem, we also make use of our former solutions for the reflection and
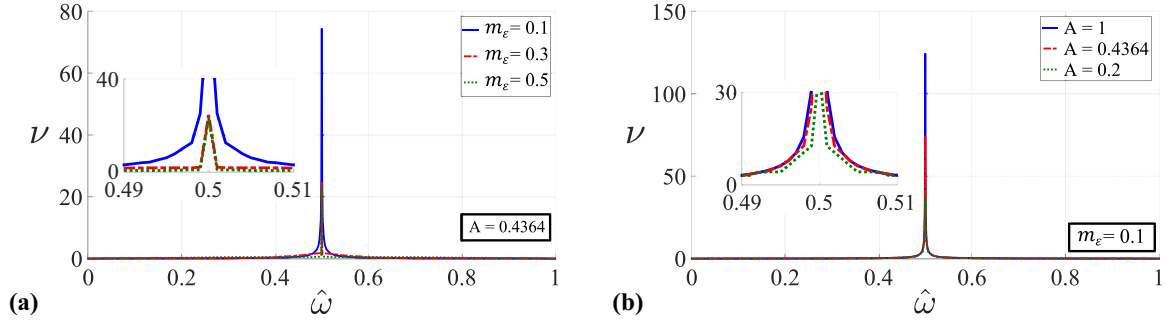
FIG. 2. Smallest eigenvalue ν of Eq. (14) as function of the reduced wave frequency $\hat{\omega} = \omega/\Omega$ for six combinations of the modulation m and the relative impedance A. (a) $A = 0.4364$ with $m_\varepsilon = 0.1,\ 0.3$, and 0.5 and (b) $m_\varepsilon = 0.1$ with $A = 0.2,\ 0.4364$, and 1.

transmission coefficients for the dynamic slab [13]. Now the question is, taking $\hat{\omega} = 1/2$, for what values of ν will these coefficients assume maximum values? Numerical solutions and comparisons between the two methods in Secs. II A and II B will be given in Secs. III and IV.

C. Weak modulation approximation

Weak modulations of the permittivity and permeability are defined by the inequalities, respectively, $m_\varepsilon \ll 1$ and $m_\mu \ll 1$. In the limits $m_\varepsilon \to 0$, $m_\mu \to 0$ (the "empty temporal lattice" approximation [13]) and considering the frequency range $0 < \hat{\omega} \leqslant 1$ and wave vector range $0 < \hat{k} \leqslant 1$, the dominant harmonics are $n = 0$ and $n = 1$ and the dominant wave vector bands are $p = 1$ and $p = 2$. With these restrictions, the set of Eq. (14) is reduced to just two equations for the amplitudes E_1 and E_2:

$$\left[A(e_{10} + \hat{\mu}_{-1}e_{11})f\left(\hat{k}_1 \frac{\nu}{2}\right)\hat{\omega} + i\hat{k}_1(\hat{\omega})f'\left(\hat{k}_1 \frac{\nu}{2}\right)e_{10} \right]E_1$$
$$+ \left[A(e_{20} + \hat{\mu}_{-1}e_{21})f\left(\hat{k}_2 \frac{\nu}{2}\right)\hat{\omega} \right.$$
$$\left. + i\hat{k}_2(\hat{\omega})f'\left(\hat{k}_2 \frac{\nu}{2}\right)e_{20} \right]E_2 = 0, \quad (15)$$

$$\left[A(\hat{\mu}_1 e_{10} + e_{11})f\left(\hat{k}_1 \frac{\nu}{2}\right)(\hat{\omega} - 1) + i\hat{k}_1(\hat{\omega})f'\left(\hat{k}_1 \frac{\nu}{2}\right)e_{11} \right]E_1$$
$$+ \left[A(\hat{\mu}_1 e_{20} + e_{21})f\left(\hat{k}_2 \frac{\nu}{2}\right)(\hat{\omega} - 1) \right.$$
$$\left. + i\hat{k}_2(\hat{\omega})f'\left(\hat{k}_2 \frac{\nu}{2}\right)e_{21} \right]E_2 = 0. \quad (16)$$

The approximate eigenvalues are obtained by setting to zero the (two by two) determinant of the coefficients of E_1 and E_2. The result turns out especially simple for $\hat{\omega} = 1/2$:

$$\left(\frac{A^2 - 1}{A^2 + 1}\right)\cos\left(\frac{\nu}{2}\right) \pm \cos\left(\frac{\nu}{8}M\right) = 0, \quad (17)$$

where the $+$ and $-$ signs give rise to the symmetric and antisymmetric electric fields, respectively, in the slab and

$$M = \left(m_\varepsilon^2 - 2m_\varepsilon m_\mu \cos\theta + m_\mu^2\right)^{1/2}. \quad (18)$$

The resonance values of ν thus depend on only two parameters: the relative impedance A, defined in Eq. (12), and the new "modulation parameter" M. Interestingly, the solutions for ν do not depend separately on m_ε, m_μ, and θ. In particular, interchanging the values of m_ε and m_μ makes no difference.

Consider first the special case of equal, in-phase modulations, $m_\varepsilon = m_\mu$ and $\theta = 0$. Then $M = 0$ and Eq. (17) reduces to

$$\cos\left(\frac{\nu}{2}\right) = \pm\left(\frac{1 + A^2}{1 - A^2}\right). \quad (19)$$

The right-hand side being greater than 1, there are no solutions—and no resonances. In Ref. [13] we found that, in this special case, there are no k gaps, either. This suggests that the resonances are intimately associated with these gaps, which was also concluded in Ref. [16] in the absence of magnetic modulation ($m_\mu = 0$).

A particularly simple situation results when the average impedance of the slab medium is equal to the impedance of the bounding medium, $A = 1$. Then Eq. (17) becomes $\cos(M\nu/8) = 0$, which has the solutions

$$\nu = \frac{4\pi}{M}, \frac{12\pi}{M}, \frac{20\pi}{M}, \ldots. \quad (20)$$

In this case of impedance matching *in the average* the solutions for ν are equidistant and inversely proportional to the modulation M.

Figures 3(a) for $M = 0.162$ and 3(b) for $M = 0.2$ show vividly how the solutions for ν can be obtained from the intersections of the two cosine functions in Eq. (17). In each of these figures, three values of the parameter A are considered, including the case $A = 1$, giving rise to the horizontal line through the origin with the solutions of Eq. (20). Figure 3(c) also demonstrates the actual resonances of the zero-order transmission coefficient (for light transmitted at the same frequency as the incident light) corresponding to Fig. 3(b), modulation $M = 0.2$, and small absorption. It is this absorption that gives rise to the bandwidths in ν. The resonances decrease in intensity with increasing values of ν.

Figures 3(a) and 3(b) suggest how to estimate the smallest resonance value of ν. It is given by

$$\pm\cos\left(\frac{\nu_{\min}}{8}M\right) \cong \frac{A^2 - 1}{A^2 + 1}. \quad (21)$$

For $A \ll 1$ this reduces to the simple result

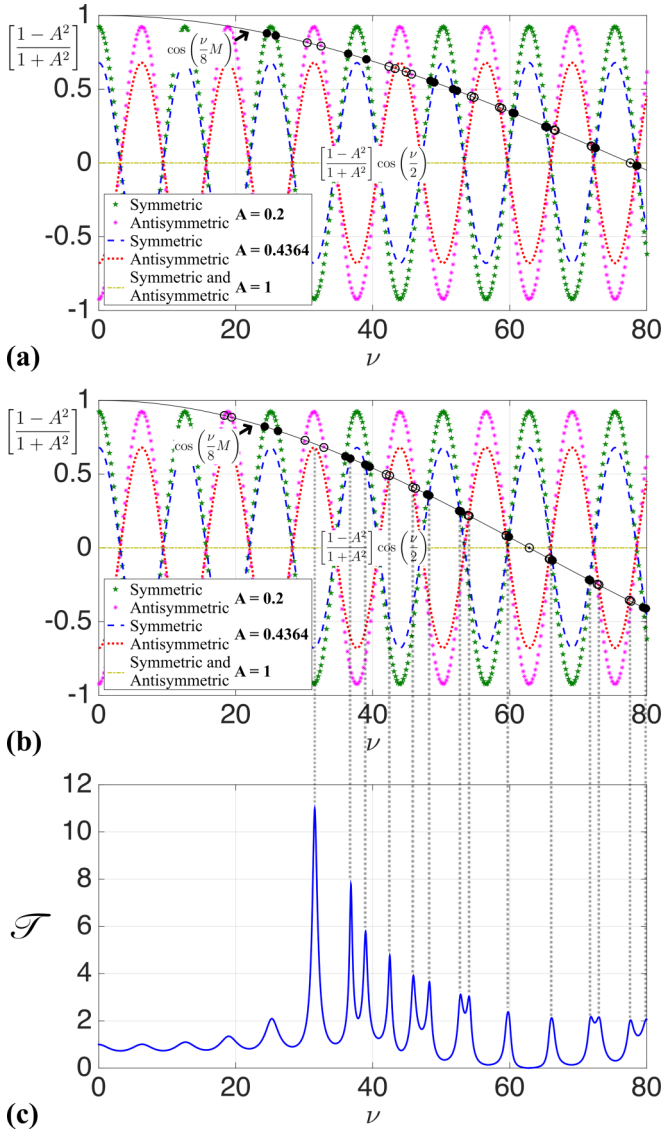$$\nu_{\min} \cong \frac{16A}{M}. \quad (22)$$

(a)

(b)

(c)

FIG. 3. Solutions of Eq. (17) for symmetric $E(x, t)$ fields (black dots) and antisymmetric $E(x, t)$ fields (circles) for $\omega = \Omega/2$ and modulations (a) $M = 0.162$ and (b) $M = 0.2$. In both (a) and (b) the intersections of the two cosine functions in Eq. (17) are given for $A = 0.2$, 0.4364, and 1 (horizontal line through origin). In (c) the resonances of the zero-order transmission coefficient are shown, corresponding to the case $M = 0.2$ and $A = 0.4364$, allowing for small absorption [$\mathrm{Im}(\varepsilon_r) = 0.01$ and $\mathrm{Im}(\mu_r) = 0.01$].

III. NUMERICAL RESULTS FOR THE PARAMETER ν

The former section emphasized the centrality of the parameter ν for the parametric resonances in a dynamic-periodic slab. In Secs. II A, II B, and II C we developed three methods to calculate ν: an exact method based on a classical eigenvalue approach to resonance, resulting in Eq. (14), another exact method based on optical response, see Ref. [13], and an approximate method for weak modulations; see Eq. (17). In Tables I–III we compare the lowest ν values obtained by these three methods for three values of the relative impedance A (same values as considered in Fig. 3). It is seen that there is excellent agreement between the two exact methods

TABLE I. Comparison of values of the ν parameters calculated by three methods: Eq. (14), Eq. (17), and Ref. [13] for 14 combinations of the parameters m_ε, m_μ, and θ. The impedance parameter is assumed to be $A = 1$.

| | | | | ν | | |
m_ε	m_μ	θ	Solution of eigenvalue equation (14)	Solution for weak mod., Eq. (17)	Calculation of transmission coefficient	Order of ν
0.1	0	0	122.66	125.66	122.63	1
0	0.1	0	122.66	125.66	122.63	1
0.2	0.1	0	123.98	125.66	123.99	1
0.2	0	0	60.00	62.83	60.27	1
0.3	0.1	0	61.04	62.83	61.04	1
0.3	0	0	41.49	41.88	41.49	1
0	0.5	0	22.91	25.13	22.89	1
0.9	0	0	12.56	13.96	12.66	1
0.1	0.1	π	59.63	62.83	59.56	1
0.1	0.1	$\pi/2$	85.02	88.85	85.3	1
0.5	0.5	π	15.62	12.56	15.39	1
0.5	0.5	$\pi/2$	17.64	17.77	17.34	1
0.9	0.9	π	5.11	6.98	5.31	1
0.9	0.9	$\pi/2$	12.58	9.87	12.56	1

and surprisingly good agreement between the approximate method and the exact ones, with the exception of modulations m close to 1. The general tendency is for $\nu_{\min}$ to diminish as the modulation becomes stronger, implying that, for a given modulation frequency, the resonance can be achieved for a thinner slab. We also note that all three tables give identical approximate results for three combinations of the parameters $(m_\varepsilon, m_\mu, \theta)$: (a) (0.2, 0, 0), (b) (0.3, 0.1, 0), and (c) (0.1, 0.1, π). That is so because the parameter M, defined by Eq. (18), has the same value in these three cases and, according to Eq. (17), ν depends only on M. This conclusion, however, does not extend to the exact results, implying that the precise dependence on m_ε, m_μ, and θ is more subtle.

TABLE II. As in Table I, for $A = 0.4364$.

| | | | | ν | | |
m_ε	m_μ	θ	Solution of eigenvalue equation (14)	Solution for weak mod., Eq. (17)	Calculation of transmission coefficient	Order of ν
0.1	0	0	74.53	74.40	74.53	3
0	0.1	0	74.51	74.40	74.51	3
0.2	0.1	0	75.22	74.40	75.22	3
0.2	0	0	37.00	36.76	37.00	1
0.3	0.1	0	37.48	36.76	37.48	1
0.3	0	0	24.59	24.24	24.59	1
0	0.5	0	23.25	22.48	23.25	3
0.9	0	0	11.74	10.58	11.74	1
0.1	0.1	π	36.82	36.76	36.82	1
0.1	0.1	$\pi/2$	49.73	49.57	49.73	1
0.5	0.5	π	10.63	10.28	10.63	1
0.5	0.5	$\pi/2$	17.15	16.14	17.15	3
0.9	0.9	π	9.00	8.44	8.95	2
0.9	0.9	$\pi/2$	12.50	13.70	12.46	4

TABLE III. As in Table I, for $A = 0.2$.

m_ε	m_μ	θ	ν Solution of eigenvalue equation (14)	Solution for weak mod., Eq. (17)	Calculation of transmission coefficient	Order of ν
0.1	0	0	37.26	37.19	37.26	1
0	0.1	0	37.25	37.19	37.25	1
0.2	0.1	0	37.61	37.19	37.61	1
0.2	0	0	24.35	24.19	24.35	3
0.3	0.1	0	24.69	24.19	24.69	3
0.3	0	0	12.29	12.10	12.29	1
0	0.5	0	11.76	11.35	11.76	3
0.9	0	0	11.93	10.32	11.93	3
0.1	0.1	π	24.23	24.19	24.23	3
0.1	0.1	$\pi/2$	24.83	24.74	24.82	1
0.5	0.5	π	10.48	10.10	10.48	3
0.5	0.5	$\pi/2$	17.18	16.04	17.18	5
0.9	0.9	π	9.89	8.62	9.89	2
0.9	0.9	$\pi/2$	12.87	14.19	12.88	4

Figure 4 gives a good general idea about the dependence on M of the three lowest ν values, as predicted by Eq. (17) and, again, for the three values of A considered in the tables. We see that ν diverges as $M \to 0$; this confirms that there are no resonances when there are no gaps between the k bands. The steplike structure in Figs. 4(b) and 4(c) can be traced to transitions between symmetric and antisymmetric fields $E(x, t)$; see Figs. 3(a) and 3(b).

The importance of the phase difference θ between the magnetic and electric modulations (assuming that $m_\varepsilon = m_\mu$) is investigated in Fig. 5. As seen, ν increases rapidly with decreasing phase difference. This figure also reconfirms the excellent accord between our three methods of calculation.

IV. TRANSMISSION AND REFLECTION COEFFICIENTS

In Fig. 3(c) we pictured the fundamental (zero-order) transmission coefficient for the frequency $\omega = \Omega/2$ as a function of the thickness parameter ν. A series of resonances was obtained, as manifested in peaks of diminishing amplitude as ν increases. In the present section we use the results of Ref. [13] to provide additional information on the parametric resonances. In addition to the fundamental transmission coefficient (order $n = 0$), in Fig. 6 we also provide results for the order $n = 1$, -1, and 2 transmission and reflection coefficients as functions of the reduced frequency $\hat\omega$. Here, the resonance parameter has been restricted to the value $\nu = 41.49$ and allowance has been made for minor absorption (small imaginary parts of $\hat\varepsilon_r$ and $\hat\mu_r$). It is notable that the parametric resonance at $\hat\omega = 1/2$ is obtained for all the harmonics n and for the reflectance, as well as transmittance. In addition, in the background, Fabry-Pérot–like oscillations appear.

In Fig. 7 we compare the zero-order transmission spectrum for weak modulation ($m = 0.1$) with the corresponding spectrum for the unmodulated slab. In the latter case, the resonance peak is, of course, missing. As for the Fabry-Pérot oscillations, these are remarkably similar to the off-resonance
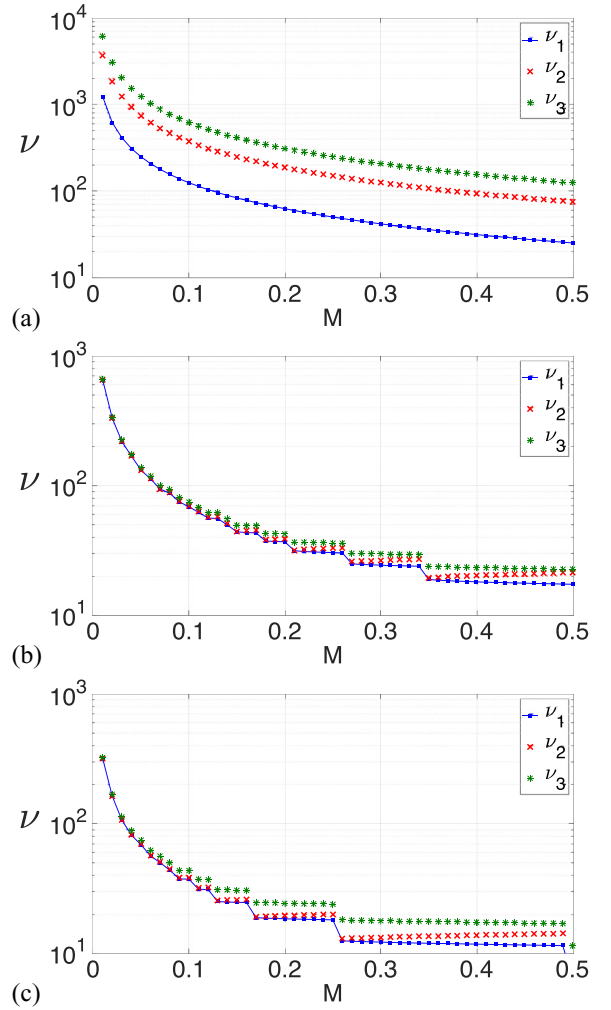

(a)

(b)

(c)

FIG. 4. First three values of the resonance parameter ν, in the weak modulation approximation, as function of the modulation parameter M, defined in Eq. (18). (a) $A = 1$, (b) $A = 0.4364$, and (c) $A = 0.2$.

oscillations in the presence of modulation. This justifies their interpretation as "Fabry-Pérot–like oscillations."

The phases of the transmission and reflection coefficients corresponding to Fig. 6 are shown in Fig. 8. The abrupt
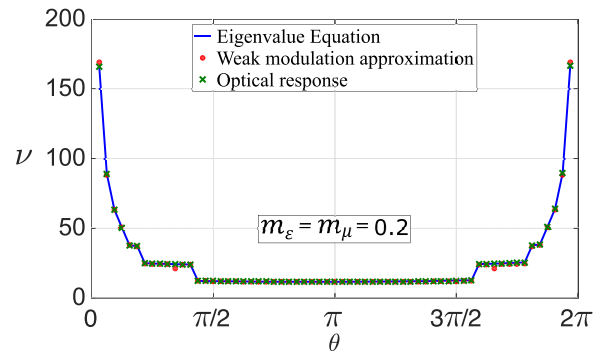

FIG. 5. Smallest ν value as function of the phase difference θ between the modulations of $\mu(t)$ and $\varepsilon(t)$, assuming that they are equal. Three methods of calculation of ν are compared.
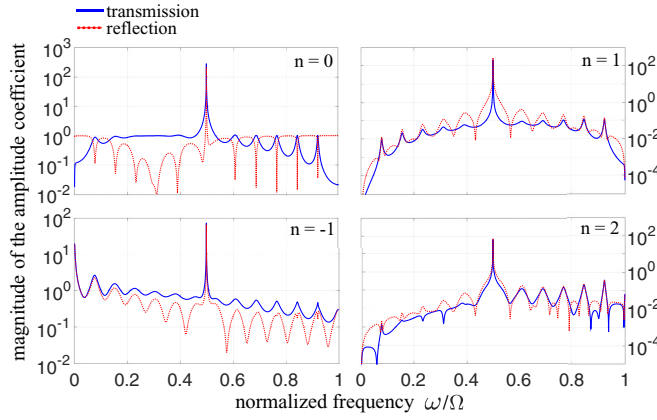
FIG. 6. Magnitude of transmission and reflection coefficients as function of reduced frequency for the harmonics $n = 0$, 1, -1, and 2. The parameter values are $\nu = 41.49$, $m_\varepsilon = 0.3$, $m_\mu = 0$, and $A = 1$.

phase changes are directly related to maxima and minima in the magnitude of the transmission and reflection coefficients. These phase transitions occur between the values 0, $\pm 1/2$, ± 1, with the exception of the case $\hat{\omega} = 1/2$.

It is also interesting to inquire, if we fix the thickness parameter ν, the impedance parameter A, and the modulation parameters $m_\varepsilon = m_\mu$, are resonances obtained for some values of the phase difference θ between the magnetic $\mu(t)$ and electric $\varepsilon(t)$ modulations? Indeed, Fig. 9 displays transmission peaks at two values of θ for each of the three sets of parameters ν and m. Absorption is neglected in (a), while small imaginary parts added to $\bar{\varepsilon}_r$ and $\bar{\mu}_r$ cause broadening in (b). These structures display no symmetry.

V. CONCLUSIONS

In this paper we explored resonances in a dynamic-periodic slab whose permittivity and/or permeability vary periodically in time, namely, a temporal photonic crystal. These resonances are strongest when the frequency of the excitation is $1/2$, or $3/2$, etc. of the modulation frequency. As shown
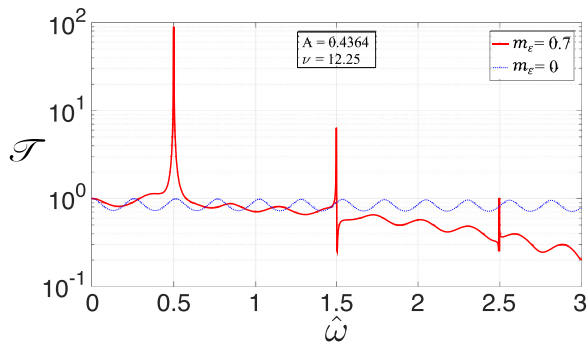

FIG. 7. Transmission spectrum of the fundamental harmonic ($n = 0$) for the first three resonances (at $\omega = \Omega/2$, $3\Omega/2$, and $5\Omega/2$). The parameter values are $\nu = 12.25$, $A = 0.4364$, $m_\varepsilon = 0.7$, and $\text{Im}(\varepsilon_r) = 0.01$. Off the strong parametric resonances the spectra resemble Fabry-Pérot resonances, which are also shown for the unmodulated ($m_\varepsilon = 0$) slab.
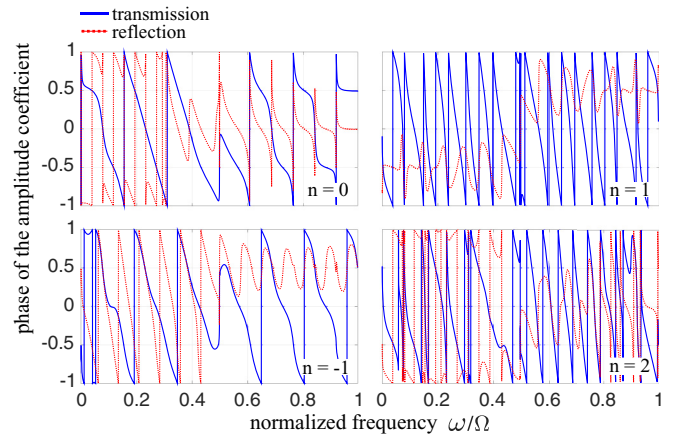

FIG. 8. Phase of transmission and reflection coefficients corresponding to Fig. 6.

in Ref. [17], precisely for these frequencies, the waves are stationary. However, an additional, geometric, condition has to be fulfilled: the parameter ν, given by Eq. (13), must assume one of a series of special ("resonant") values that depend, principally, on a modulation parameter M, given by Eq. (18), and on the relative impedance, Eq. (12). These resonances occur when the electric field in the slab is either symmetric or antisymmetric with respect to the slab's center. We presented two methods for exact calculations of ν: as a solution of an eigenvalue problem and as derivation of the optical response for the slab. The results of these calculations
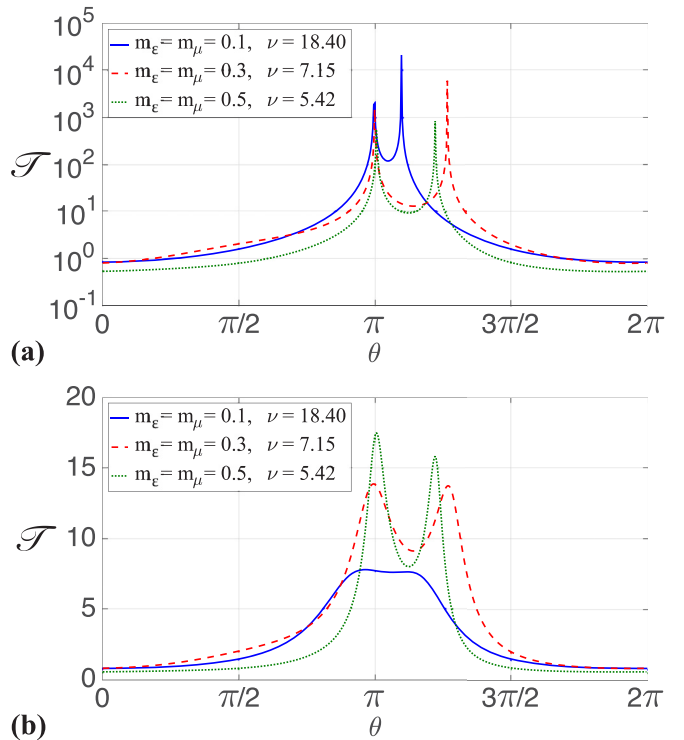

FIG. 9. Zero-order ($n = 0$) transmission coefficient as function of phase difference θ without (a) and with (b) absorption [$\text{Im}(\varepsilon_r) = 0.01$ and $\text{Im}(\mu_r) = 0.01$]. Here, $A = 0.2$.

are in excellent agreement. The resonances occur not only for the fundamental response, but also for harmonics such as $\omega \pm \Omega$, $\omega \pm 2\Omega$, etc. and in both the reflectance and the transmittance. We also developed an approximate method, appropriate for weak modulation, $M \ll 1$. Surprisingly, as long as M is not quite near to 1, this method predicts ν values in reasonable agreement with the accurate calculations. It also reveals that values of the electric and magnetic modulations, m_ε and m_μ, and the phase difference θ between these modulations affect the resonances only through M, Eq. (18), as long as $M \lesssim 0.5$. In addition to the resonances in the amplitudes of the transmission and reflection coefficients, they also reveal Fabry-Pérot–like oscillations. Moreover, the phases of these coefficients display corresponding abrupt transitions. As can be expected, small imaginary parts, added to the

average permittivity and permeability, cause broadening of the resonance lines.

Modulated low-pass transmission lines being intimately related to temporal photonic crystals [14,15], we expect that the resonance effects predicted in the present paper can be realized experimentally for long-wavelength waves in periodically modulated, low-absorption transmission lines. Similar resonance phenomena can be also expected in other modulated systems, such as a slab whose elastic constants and/or mass density are periodic functions of time.

[1] B. W. Plansinis, W. R. Donaldson, and G. P. Agrawal, Phys. Rev. Lett. **115**, 183901 (2015).

[2] B. W. Plansinis, W. R. Donaldson, and G. P. Agrawal, J. Opt. Soc. Am. B **33**, 1112 (2016).

[3] J. Zhou, G. Zheng, and J. Wu, Phys. Rev. A **93**, 063847 (2016).

[4] M. Castellanos Muñoz, A. Y. Petrov, L. O'Faolain, J. Li, T. F. Krauss, and M. Eich, Phys. Rev. Lett. **112**, 053904 (2014).

[5] M. Notomi and S. Mitsugi, Phys. Rev. A **73**, 051803 (2006).

[6] H. Ramezani, P. K. Jha, Y. Wang, and X. Zhang, Phys. Rev. Lett. **120**, 043901 (2018).

[7] K. A. Lurie and V. V. Yakovlev, IEEE Antennas Wirel. Propag. Lett. **15**, 1681 (2016).

[8] A. R. Mkrtchyan and A. G. Hayrapetyan, Mod. Phys. Lett. B **24**, 1951 (2010).

[9] N. Chamanara, S. Taravati, Z.-L. Deck-Léger, and C. Caloz, Phys. Rev. B **96**, 155409 (2017).

[10] S. Taravati, N. Chamanara, and C. Caloz, Phys. Rev. B **96**, 165144 (2017).

[11] D. Correas-Serrano, J. S. Gomez-Diaz, D. L. Sounas, Y. Hadad, A. Alvarez-Melcon, and A. Alù, IEEE Antennas Wirel.

Propag. Lett. **15**, 1529 (2016); D. Ramaccia, D. L. Sounas, A. Alù, F. Bilotti, and A. Toscano, IEEE Trans. Antennas Propag. **63**, 5593 (2015); Y. Hadad, J. C. Soric, and A. Alù, Proc. Natl. Acad. Sci. U.S.A. **113**, 3471 (2016); S. Taravati and C. Caloz, IEEE Trans. Antennas Propag. **65**, 442 (2017).

[12] J. R. Zurita-Sánchez, P. Halevi, and J. C. Cervantes-González, Phys. Rev. A **79**, 053821 (2009).

[13] J. S. Martínez-Romero, O. M. Becerra-Fuentes, and P. Halevi, Phys. Rev. A **93**, 063813 (2016).

[14] J. R. Reyes-Ayona and P. Halevi, Appl. Phys. Lett. **107**, 074101 (2015).

[15] J. R. Reyes-Ayona and P. Halevi, IEEE Trans. Microwave Theory Tech. **64**, 3449 (2016).

[16] J. R. Zurita-Sánchez and P. Halevi, Phys. Rev. A **81**, 053834 (2010).

[17] J. S. Martínez-Romero and P. Halevi, Phys. Rev. A **96**, 063831 (2017).

[18] J. R. Zurita-Sánchez, J. H. Abundis-Patiño, and P. Halevi, Opt. Express **20**, 5586 (2012).